Article

The Role of Deregulated MicroRNAs in Age-Related Macular Degeneration Pathology

Hanan ElShelmani[1,2], Michael A. Wride[1], Tahira Saad[2], Sweta Rani[3], David J. Kelly[4], and David Keegan[2]

[1] Ocular Development and Neurobiology Research Group, Zoology Department, School of Natural Sciences, University of Dublin, Trinity College Dublin, Dublin 2, Ireland
[2] Mater Retina Research Group, Mater Misericordiae University Hospital, Eccles St., Dublin 7, Ireland
[3] Department of Science, Waterford Institute of Technology, Waterford, Ireland
[4] Zoology Department, School of Natural Sciences, University of Dublin, Trinity College Dublin, Ireland

Correspondence: David Keegan, Mater Misericordiae University Hospital, Eccles St., Dublin 7, Ireland. e-mail: dkeegan@mater.ie

Purpose: We previously identified three microRNAs (miRNAs) with significantly increased expression in the serum of patients with age-related macular degeneration (AMD) compared with healthy controls. Our objective was to identify potential functional roles of these upregulated miRNAs (miR-19a, miR-126, and miR-410) in AMD, using computational tools for miRNAs prediction and identification, and to demonstrate the miRNAs target genes and signaling pathways. We also aim to demonstrate the pathologic role of isolated sera-derived exosomes from patients with AMD and controls using in vitro models.

Methods: miR-19a, miR-126, and miR-410 were investigated using bioinformatic approaches, including DIANA-mirPath and miR TarBase. Data on the resulting target genes and signaling pathways were incorporated with the differentially expressed miRNAs in AMD. Apoptosis markers, human apoptosis miRNAs polymerase chain reaction arrays and angiogenesis/vasculogenesis assays were performed by adding serum-isolated AMD patient or control patient derived exosomes into an in vitro human angiogenesis model and ARPE-19 cell lines.

Results: A number of pathways known to be involved in AMD development and progression were predicted, including the vascular endothelial growth factor signaling, apoptosis, and neurodegenerative pathways. The study also provides supporting evidence for the involvement of serum-isolated AMD-derived exosomes in the pathology of AMD, via apoptosis and/or angiogenesis.

Conclusions: miR-19a, miR-126, miR-410 and their target genes had a significant correlation with AMD pathogenesis. As such, they could be potential new targets as predictive biomarkers or therapies for patients with AMD.

Translational Relevance: The functional analysis and the pathologic role of altered miRNA expression in AMD may be applicable in developing new therapies for AMD through the disruption of individual or multiple pathophysiologic pathways.

Introduction

Age-related macular degeneration (AMD) is a common eye condition and one of the leading causes of progressive visual impairment among the elderly population; the prevalence of AMD is increasing.[1] A normally functioning retinal pigment epithelium (RPE) is fundamental for vision. The RPE protects the retina as part of the blood–retina barrier. The ability of photoreceptors to function properly depends on the interaction between the RPE and photoreceptor cells.[2] RPE disorders can lead to photoreceptor degeneration and RPE dysfunction is implicated in AMD pathogenesis.[3]

MicroRNAs (miRNAs) participate in signaling networks; miRNAs can be released into the extracellular fluid and transported to target cells via vesicles, such

as exosomes, or directly by binding to proteins.[4] Large numbers of miRNAs have been discovered in humans, and each miRNA may have several gene targets. Such target genes have been implicated in cell cycle regulation, cell function signaling, migration, proliferation, and neural cell fate. Signaling pathways are important in human physiologic functioning, and their disruption or malfunction can result in diseases.[5] miRNA expression is significantly dysregulated in the majority of human diseased tissue compared with normal tissue, such as cancer, inflammation, diabetes, cardiovascular disease, and neurologic disorders.[6,7] Several target genes of miRNAs also further regulate physiologic and pathologic responses.[8,9]

A number of circulating miRNAs have been identified as potential agents for development and/or progression of AMD.[9] A recent study showed that miR-486-5p and miR-626 had greater expression in the serum of patients with AMD compared with the control group, whereas miR-885-5p was significantly downregulated in AMD patient groups.[10] These miRNAs are known to have essential roles in apoptosis and neovascularization pathways, which have a role in the pathogenesis of AMD.[10] miR-27a, miR-146a, and miR-155 are also suggested to play an important role in AMD. Furthermore, amyloid-β retinal deposition leads to inflammatory and apoptotic events along with differential expression of miRNAs which in turn leads to transforming growth factor-β pathway dysregulation. In addition, miR-155 and miR-27a have been shown to target 42 genes involved in the transforming growth factor-β pathway (DIANA-miRPath), whereas miR-146a can target genes involved in inflammatory pathways (Toll-like receptor), nuclear factor-κB, tumor necrosis factor signaling pathways).[9,11]

Genetic and bioinformatic analyses can be used to further enhance our understanding of the function of miRNAs in AMD.[12] Target gene and signaling pathway correlation with the expression of miRNAs may increase our understanding of AMD pathology. Such an approach is more powerful than miRNA expression testing alone.[8,13] However, the interpretation of computational predictions of miRNA targets and signaling pathways is challenging, as the current tools for target prediction are based on gene-level activity.[13] These miRNA-related database systems provide further insight into miRNAs and their target genes.[14] miRNAs have several target genes and regulatory functions, and so the biological role of miRNAs and their therapeutic potential need to be further explored by the integration of computational and experimental approaches.[13]

In AMD, pathways related to the wound response, the complement cascade, and cell survival have been identified. Early AMD pathogenesis has significant activation of promitotic pathways, which is associated with differentiation and cell proliferation events.[15] That study also discovered a new global pathway with activation signatures of AMD involved in the cell-based inflammatory response: IL-2, STAT3, and ERK.[15] Alzheimer's disease (AD) and AMD are multifactorial and progressive inflammatory degenerations and are considered to be neurodegenerative diseases. The most recent data show that 4 miRNAs (miRNA-9, miRNA-125b, miRNA-146a, and miRNA-155) were upregulated in these neurodegenerative diseases. These upregulated miRNAs consequently downregulate complement factor H expression, a major inhibitor of the innate immune and inflammatory reaction, the inflammatory pathology that is involved in both AMD and AD. It has been demonstrated that the retina in AMD has an abundance of upregulated miR-9, miR-125b, miR-146a, and miR-155, which are common in the complement factor H deficiency that causes inflammatory neurodegeneration.[16] The expression of miRNA-7, miRNA-9-1, miRNA-23a/miRNA-27a, miRNA-34a, miRNA-125b-1, miRNA-146a, and miRNA-155 is significantly increased in both the AD-affected superior temporal lobe neocortex and the AMD-affected macular region of the retina.[16] Other observational studies also provided evidence for the role of miRNAs (miRNA-9, miRNA-34a, miRNA-125b, miRNA-146a, and miRNA-155) in AD and AMD pathogenesis.[17,18]

miRNAs play critical roles in the processes of AMD pathology. Several miRNAs, involved in choroidal neovascularization or RPE atrophy, are considered to be AMD therapeutic targets.[9] Choroidal neovascularization can be induced by angiogenic factors, which are produced from apoptotic RPE and inflammatory cells. Anti-vascular endothelial growth factor (anti-VEGF) therapy is an essential treatment for neovascular AMD.[19] A group of specific miRNAs (angiomiRs) have been demonstrated to play a major role in angiogenesis. These miRNAs include the miR-15/107 group, the miR-17~92 cluster, miR-21, miR-132, miR-296, miR-378, and miR-519c. It has also been shown that there is an increased expression of apoptosis-inducing ligands on the photoreceptors of patients with exudative AMD or geographic atrophy. Apoptosis is believed to be increased by miR-23a inhibition and decreased by an miR-23a mimic.[9,20] Drusen are a hallmark of AMD; they are a common early sign and are a risk factor for developing dry AMD. An aged RPE of an

AMD patient is believed to be more susceptible to genetic mutations owing to the alteration of biological processes.[21] Drusen formation is hypothesized to result from the release of intracellular proteins via exosomes by the old RPE. In addition, drusen in AMD donor eyes contain exosome markers CD63, CD81, and LAMP2.[21]

Exosomes are 50- to 90-nm membrane microvesicles,[22] released by several cell types, including tumor cells.[23] Exosomes contain genetic materials, such as messenger RNAs and miRNAs, which play an important role in cell–cell communication. They are secreted into the extracellular space by cells in both physiologic and pathologic situations, including pathologic angiogenesis, the oxidative stress response, immune response, inflammation, and oncogenesis. The ability of cells to uptake exosomes has been confirmed by using confocal microscopy.[24] In vitro and in vivo studies have revealed that exosome transfer from cell to cell mediates disease progression. For instance, exosomes have a key role in tumor progression as a result of the capability of tumor cell–derived exosomes to change the host microenvironment, which leads to tumor cell growth and disease progression.[25] Moreover, miRNAs transferred via exosomes may mediate epigenetic transfer of tumor clones through miRNA molecules.[24] Exosome markers have also been found in the region of Bruch's membrane in the retinas of old mice; they were also upregulated in RPE cells exposed to rotenone (inducing mitochondrial DNA damage).[21,26] Another study has revealed that mesenchymal stem cell-derived exosomes may inhibit tumor growth in vitro and in vivo by downregulating VEGF expression in tumor cells.[27] Thus, the function of exosomal miRNAs in host target cells provides a novel therapeutic gene delivery system.[28]

The objective of this study was to identify the potential pathologic role of miRNAs in AMD using computational tools for miRNAs prediction and identification and in vitro functional studies using exosomes to deliver miRNAs.

Methods

Study Population

Patients with AMD and controls were recruited for the study from the Mater Private Hospital, Mater Misericordiae University Hospital (MMUH), Dublin, Ireland, and the Waterford Institute of Technology, Waterford, Ireland. The patients with AMD were a part of the CARMA (Carotenoids in Age-Related Maculopathy) study.[29] Informed consent was obtained from the subjects after explanation of the nature and possible consequences of the study. Ethical approval for the study was obtained from MMUH which conformed to the tenets of the Declaration of Helsinki.

In total, 80 patients with clinically documented AMD were enrolled in this study: 40 with dry AMD and 40 with wet AMD. Forty healthy individuals were enrolled as controls (i.e., no signs or symptoms of AMD), giving a total of 120 individuals participating in the study (dry AMD [$n = 40$], wet AMD [$n = 40$], and controls [$n = 40$]). miR-126, miR19a, and miR-410 expression were quantified as described previously.[30]

Bioinformatics

Total RNA isolation was carried out from sera of patients with AMD and controls ($n = 120$). There were 377 miRNAs that were co-analyzed and validated using array technologies. Three miRNAs (miR-126, miR-19a, and miR-410) were confirmed by quantitative real-time polymerase chain reaction (PCR), and significantly increased quantities were found in serum of patients with AMD compared with healthy controls. The association between miRNAs and KEGG pathways was calculated through the A web-server DIANA-miRPath.[31] A web-based computational tool (DIANA-mirPath micro-T 4.0) was used to identify potential protein coding messenger RNA targets and potential molecular pathways that are altered by the differentially expressed miRNAs. The following miRNAs were analyzed: miR-126, miR-19a, and miR-410. The predicted targets were identified from DIANA-miRpath software using the miRtarBase algorithm. The miRTarBase database was also used to recognize the target genes of the three validated miRNAs.

miRNA Target Genes and Signaling Pathway Integration

The detected miRNA gene targets were integrated manually with their signaling pathways using KEGG (Kyoto Encyclopedia of Genes and Genomes) Pathways enrichment.

Exosome Isolation and Quantification

Exosomes were isolated from 250 µL of serum using ExoQuick Exosome Precipitation (Systems Biosciences, Stratech, UK) according to the manufacturer's instructions. Exoquick is suitable for the extraction of exosomes from small samples, such as serum samples.[32] Exosomes were isolated from a total of

36 samples (12 patients with dry AMD and12 patients with wet AMD, and 12 controls). We transferred 250 µL of serum into a sterile vessel and 63 µL of ExoQuick Exosome Precipitation were added, and then mixed well by inverting or flicking the tube. The mix was incubated at room temperature for 30 minutes and the ExoQuick/serum mixture was then centrifuged at 1500*g* for 30 minutes. Centrifugation was performed at 4°C. After centrifugation, the exosomes may appear as a white pellet at the bottom of the vessel. The supernatant was aspirated, and the residual ExoQuick solution was spun down by centrifugation at 1500*g* for 5 minutes. All traces of fluid were removed by aspiration, taking great care not to disturb the precipitated exosomes. The exosome pellet was resuspended in 1/10 (25 µL) of the original volume using nuclease-free water. Isolated exosomes were stored at –80°C. Exosomes were quantified with Qubit fluorometric quantitation (Invitrogen, Paisley, UK) using 1 µL of exosome sample for each measurement as per the manufacturer's instructions.

NanoSight Particle Analysis

Analysis of the size distribution of the isolated exosome samples was performed by measuring the rate of Brownian motion using the NanoSight LM10 system (Malvern Panalytical, Mesbury, UK). Serum-derived exosome preparations were diluted to approximately 1:10,000 in phosphate-buffered saline to provide optimal measurement by the NanoSight LM10 system. The LM10-HS instrument has a high sensitivity camera which allows smaller, lower refractive index particles to be analyzed.

Western Blot Analysis to Track Exosomes With Validated Antibody Systems

Exosome antibodies for Western blot analysis (SBI, Stratech, UK) were used along with an ExoELISA kit, which allowed fast analysis of exosomal protein markers (CD63, CD9, CD81, or Hsp70) and confirmation of exosomes. The exosome pellet was isolated as previously described, centrifuged at 1500*g* for 5 minutes to remove all traces of fluid, and great care was taken not to disturb the pellet. We added 200 µL of radioimmunoprecipitation assay buffer(along with the appropriate protease inhibitor cocktail) to the exosome pellet and vortexed for 15 seconds, then placed at room temperature for 5 minutes to allow complete lysis to occur. A Qubit assay was used to determine the yield, which was 20 µg of serum exosome proteins.

Laemmli buffer (with beta-mercaptoethanol) was added and the mixture heated at 95°C for 5 minutes, then chilled on ice for 5 minutes before loading onto the gel. Standard sodium dodecyl sulphate-polyacrylamide gel electrophoresis was performed and Western transfer onto polyvinylidene difluoride membrane was carried out. The membrane was blocked with 5% dry milk in tris-buffered saline + 0.05% Tween (TBS-T) for 1 hour. The blot was then incubated overnight at 4°C with exosome-specific primary antibody (CD63, CD9, CD81, and Hsp70; SBI) at 1:1000 dilution (5% dry milk in TBS-T). The blot was washed three times with TBS-T and incubated for 1 hour at room temperature with exosome-validated secondary antibody (goat–rabbit–horseradish peroxidase; SBI) at 1:20,000 dilution (5% dry milk in TBS-T), after which the blot was washed three times with TBS-T. The blot was then incubated with a chemiluminescent substrate and visualized on the Fujifilm LAS-3000 imaging equipment system.

Cell Culture

The human retinal pigment epithelial cell line ARPE-19 was obtained from the Catherine McAuley Centre at the Mater Misericordiae University Hospital, Dublin. This cell line was maintained in Dulbecco's modified Eagle's medium supplemented with 4 mm L-glutamine, 10% fetal bovine serum, 100 U/mL penicillin and 100 µg/mL streptomycin at 37°C in 5% CO_2 in air. The culture medium was replaced at least twice weekly. In all experiments, cells were maintained at 70% to 80% confluency and seeded the day before treatment.

Western Blot Analysis

Western blotting was performed on cell lysates of exosomes derived from patients with AMD and controls and treated with ARPE-19 to determine the effect of exosomes on RPE by monitoring three apoptosis markers: polyADP-ribose polymerase (PARP), Apaf-1, and caspase 3. ARPE-19 cells were seeded in 6-well plates at a density of 2×10^5 per well with 3 mL of culture medium. The wells of each experiment were prepared in triplicate. Total cellular proteins were extracted from samples of ARPE-19 cells treated with exosomes using lysis buffer.

After washing in phosphate-buffered saline twice, cell pellets were processed for protein lysis with radioimmunoprecipitation assay buffer (Merk Millipore, Darmstadt, Germany) containing a complete protease inhibitor cocktail (Roche, Welwyn Garden City, UK). Samples were incubated at 4°C with agitation for 30 minutes and then centrifuged at 10,500 rpm

for 30 minutes at 4°C. The supernatant was aliquoted and stored at −80°C. The samples were prepared with loading buffer (Sigma Aldrich, Darmstadt, Germany) and water was added to bring all the samples to the same concentration. Parafilm was wrapped around the lids of the Eppendorf tubes to prevent evaporation and the samples were boiled at 95°C for 5 minutes. If not used immediately the samples were stored at –20°C.

Sodium dodecyl sulphate-polyacrylamide gel electrophoresis was carried out using 12% sodium dodecyl sulphate polyacrylamide gel (Sigma-Aldrich, Gillingham, UK) with the Bio-Rad (Fannin, ROI) Mini-Protean 3-cell system. Protein quantification was performed using Qubit fluorometric quantitation according to the manufacturer's protocol (Invitrogen). We placed 25 µg of protein sample in 30 µL of final volume in each well with Laemmli loading buffer (Bio-Rad). We loaded 15 µL of protein marker (ColorBurst Electrophoresis Marker; Sigma-Aldrich) as a reference for molecular weight. Unoccupied wells were loaded with Laemmli buffer for optimal running. The gel was run in a standard Tris-glycine running (migration) buffer in the Bio-Rad electrophoresis system at 100 V for 1 hour. After running, the stacking gel was removed, and the running gel was stained with Coommassie blue protein dye (Brilliant Blue R Concentrate; Sigma-Aldrich) for 4 hours at room temperature. The gel was agitated to fix and stain proteins, then washed in a mixture of 67% dH$_2$O, 8% acetic acid, and 25% methanol solution to wash away excess dye from the gel and visualize separated proteins.

Immunoblotting involved using the following primary antibodies: monoclonal anti-β-Actin peroxidase (Sigma-Aldrich), Apaf-1 (Cell Signaling 5088), PARP (Cell Signaling 9542) and, caspase 3 (Santa Cruz H-277). Enzyme chemiluminescence was used for band detection (enzyme chemiluminescence Plus Western Blotting Detection Reagents, Amersham, UK), then visualized with the Fujifilm LAS-3000 system at different exposure times ranging from 2 to 10 minutes. Images were processed for band intensity, measured for target proteins, and normalized to the endogenous control protein after every blot was carried out in triplicate. β-Actin protein expression analysis was carried out, followed by expression analysis of several targets. ImageJ densitometry software was used for quantification of western blots.

Human Apoptosis miScript miRNA PCR Array Profiling in ARPE-19 Cells Treated With AMD-Derived Exosomes

The Human Apoptosis miScript miRNA PCR Array is part of the miScript PCR System for miRNA detection and quantification (Qiagen, Manchester, UK) and profiles the expression of 84 miRNAs that regulate programmed cell death by inhibiting proapoptotic and anti-apoptotic gene expression. This array provides a convenient way to quickly analyze the miRNAs most relevant to apoptosis, the functional gene grouping, as shown in Supplementary Table S5.

Total RNA was isolated from samples using the GenElute Mammalian Total RNA Miniprep Kit (Sigma Aldrich, Gillingham, UK). Cell pellets were vortexed briefly to loosen cells. We added 250 mL of lysis solution/2-ME mixture, then pipetted thoroughly until all clumps disappeared. Lysed cells were then added into a GenElute Filtration Column, centrifuged at maximum speed (12,000g) for 2 minutes, and the filtration column then discarded. We added 500 mL of 70% ethanol solution to the filtered lysate and pipetted up and down to ensure even mixing. We pipetted 700 mL of the lysate/ethanol mixture into a GenElute Binding Column and centrifuged at maximum speed for 15 seconds. The collection tube was retained, and flow-through liquid was discarded. A series of wash steps were then performed, each of which required the introduction of wash solution to the top of the column, followed by centrifugation at maximum speed for 15 seconds. Binding columns were then transferred to fresh collection tubes, and the process was repeated. Binding columns were again transferred to fresh 2-mL collection tubes, and 50 mL of the elution solution was added before centrifugation at maximum speed for 1 minute. Elution with a second 50-mL volume of elution solution was performed, with both eluates (same sample) collected in the same tube. Purified RNA was present in the flow-through eluate (∼45 or 90 mL total). Samples were then stored at −80°C before transcription into complementary DNA.

A set of controls present on each array enables data analysis using the $\Delta\Delta CT$ method of relative quantification, assessment of reverse transcription performance and assessment of PCR performance. Using SYBR Green real-time PCR (Qiagen), the expression of a focused panel of miRNAs related to apoptosis can be easily and reliably analyzed with this miScript miRNA PCR array. Complementary DNA is prepared using the miScript II RT Kit, and the qPCR using miScript SYBR Green PCR Kit (Qiagen). Data analysis was performed using online data analysis software for miScript miRNA PCR Array, available at http://pcrdataanalysis.sabiosciences.com/mirna. Quantification of the miRNAs was performed using the $\Delta\Delta CT$ method of relative quantification. The data were normalized by SNORD68, because it was the most consistent miRNA control among the samples (Supplementary Table S1).
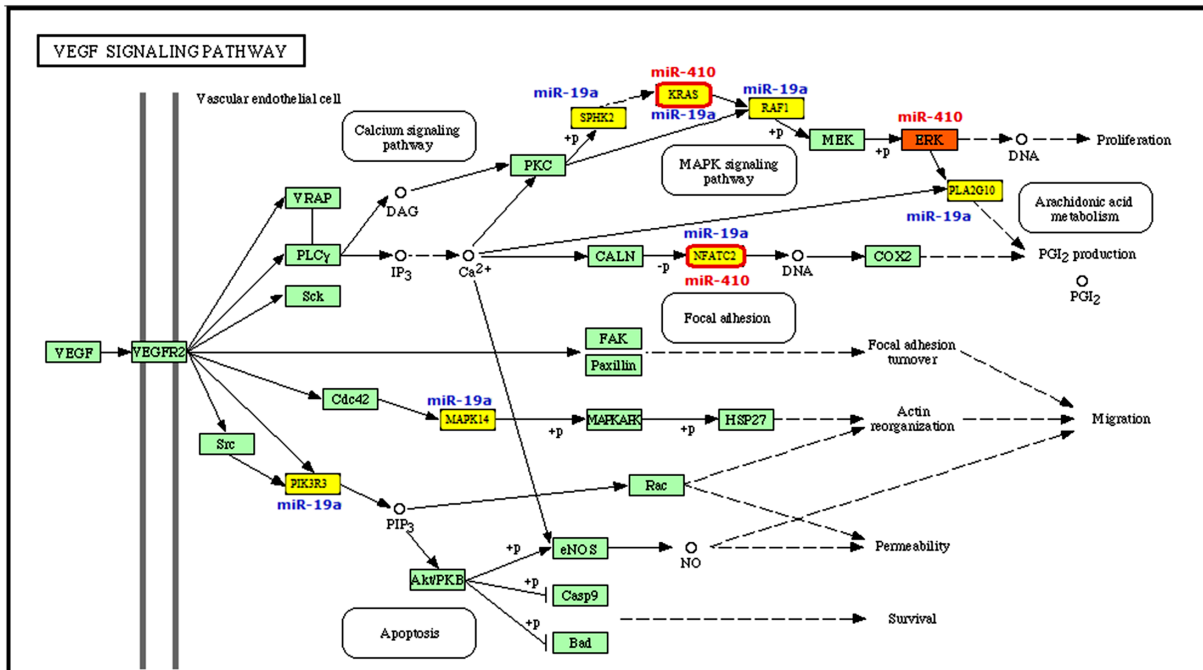
Figure 1. VEGF signaling pathway and the predicted gene targets of miR-410 (KRAS, NFATC2, ERK) and miR-19a (KRAS, MAPK1, PPP3CA, PIK3CA, NFATC2, SPHK2, PLA2G10, MAPK14, PIK3R3, RAF1) which are involved in the MAPK signaling pathway and arachidonic acid metabolism. Core image from KEGG.

Vasculogenesis Using Angiogenesis Assay

Angiogenesis assays were performed using the V2a Kit (ZHA-4000) by TCS-Cellworks (Caltag Medsystems, Buckingham, UK) according to manufacturer's instructions. On day 1, human endothelial cells were cultured in a 24-well plate. On day 2, 24 hours after seeding, cells were treated with VEGF (positive control), suramin (negative control), and 10 µg of serum-derived exosomes (neovascular AMD, atrophic AMD, and control-derived exosomes). On days 4, 6, 8, 10, and 12 (i.e., every 48 hours) the medium was changed, and cells were retreated with the additions as described as appropriate until day 14, when tubule staining was performed, and photographs were taken. The tubule-like structures were analyzed by the TCS Cellworks AngioSys Image Analysis Software (ZHA-6000, Caltag Medsystems).

Statistical Analyses

Statistical analyses were performed, to compare miRNAs in control and dry or wet AMD serum samples from age- and gender-matched donors. In the case of two-sample comparisons (wet vs. control and dry vs. control), a Student's t-test assuming unequal variances was used to determine whether there was a significant difference between the two sample means.

Differences were considered significant if the P value was 0.05 or less (denoted with a star on graphs). In the case of three-sample comparisons (wet, dry, and control), an analysis of variance test was used to determine whether there was a significant difference between the three sample means. Differences were considered significant if the P was 0.05 or less.

Results

miRNA Target Genes

The AMD-associated miRNAs that warranted further investigation were miR-19a, miR-126, and miR-410; these miRNAs showed overexpression patterns among patients with AMD.[30] The DIANA-mirPath results identified predicted targets for the altered expression of three miRNAs of interest in different signaling pathways. The miRNAs with altered expression were found to be involved in several pathways, including the VEGF signaling pathway (Fig. 1), complement and coagulation cascade (Fig. 2), apoptosis (Fig. 3), and neurodegenerative disorders (Fig. 4) as targets for the miRNAs.

miR-410 was identified as having 805 predicted target genes and was found in 173 pathways. miR-19a had 839 predicted target genes and was found in
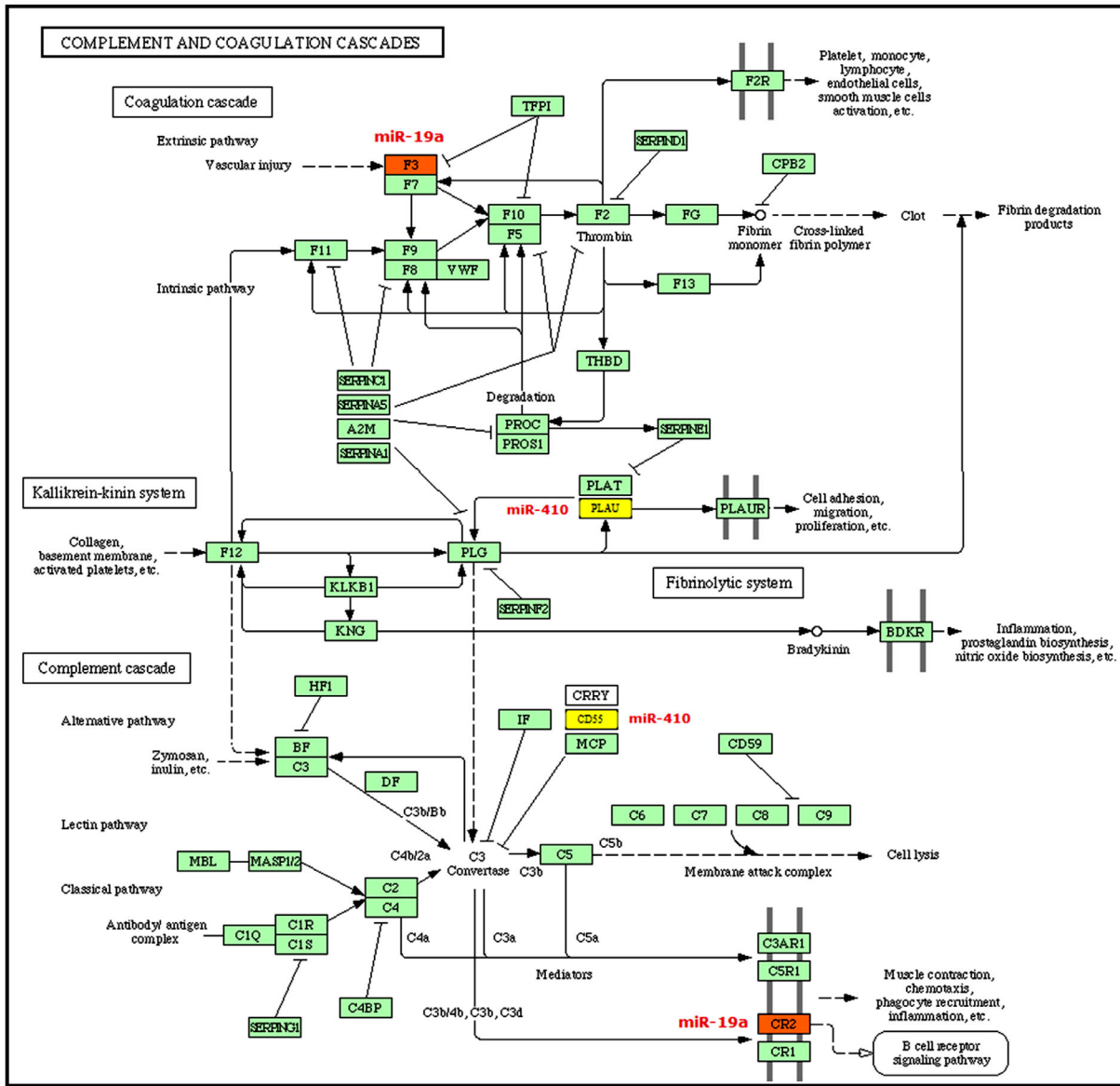
Figure 2. Complement and coagulation cascade and the predicted gene targets of miR-410 (CD55, PLAU) and miR-19a (F3, CR2), which are involved in the extrinsic pathway (vascular injury), as well as cell adhesion, migration and proliferation, B-cell receptors signaling pathway and C3 convertase formation. Core image from KEGG.

166 pathways, and miR-126 had 22 predicted target genes and was found in six pathways. miR-410 and miR-19a targets were involved in the apoptosis signaling pathway (NTRK1, IL1R1, PRKAR2B, PPP3CA, BIRC4, PIK3CA, MAP3K14, and PIK3R3) (Fig. 3; Table 1). Furthermore, the computational data also identified several miRNA gene targets that were involved in pathways, including the VEGF signaling pathway (KRAS, MAPK1, PPP3CA, PIK3CA, NFATC2, SPHK2, PLA2G10, MAPK14, PIK3R3, and RAF1), which are targeted by miR-19a and miR-410 as shown in Figure 1 and Table 1. More target genes

were found in the complement and coagulation cascade signaling pathway (CD55, PLAU, CR2, and F3) (Fig. 2), neurodegenerative signaling pathway (SOD1) (Fig. 4), nicotinate and nicotinamide metabolism (PBEF1) (Supplementary Fig. S2) and the retinol metabolism signaling pathway (ALDH1A2) (Supplementary Fig. S3) (all shown in Table 1). Target scan results identified 22 predicted target genes for miR-126, and it is involved in the cell communication pathway by targeting the ITGA6 gene (Supplementary Fig. S1; Table 1). miR-126 also targets IGF-1 in the neurodegenerative signaling pathway.
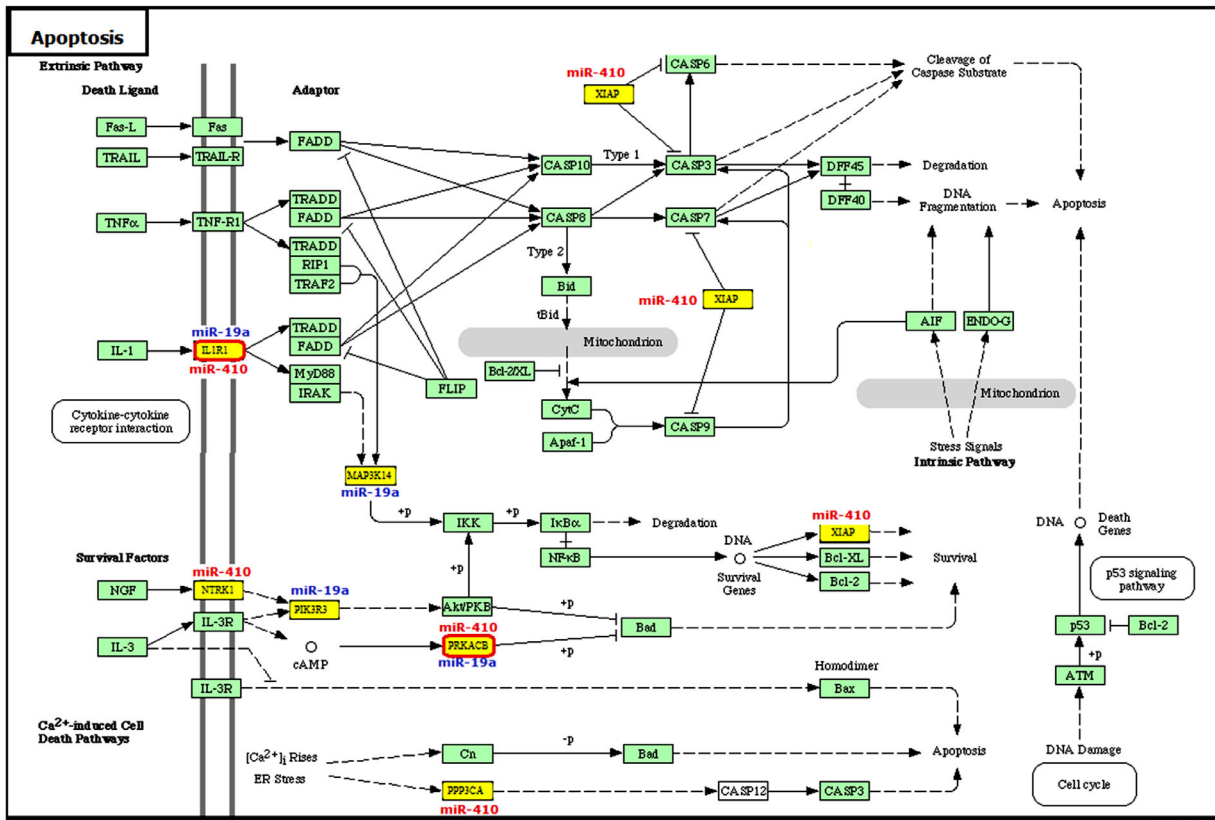
Figure 3. Apoptosis signaling pathway and the predicted gene targets of miR-410 (IL1R, XIAP, NTRK1, PPP3CA, PRKACB3) and miR-19a (IL1R1, PIK3R3, MAP3K14, PRKACB3), which are involved in cytokine–cytokine receptor interaction. Core image from KEGG.

Validation of miRNA Target Genes Using the miR TarBase Database

The miR TarBase database was used to identify the validated miRNA target genes for the three validated miRNAs, namely miR-410, miR-126, and miR-19a (see Supplementary Table S2, Supplementary Table S3, and Supplementary Table S4 for the target genes and validation methods used for the miR TarBase database).

Exosome Quantification and Confirmation

Exosome Quantification

Exosomes were isolated from a total of 36 serum samples from patients with AMD and controls (12 samples each from dry AMD, wet AMD, and control groups) and quantified with Qubit fluorometric quantitation (Invitrogen). The quantity of exosomes was found to be consistent among specimens (between 600 and 800 μg/25 μL) (Supplementary Fig. S4). Western blotting analysis results confirmed the presence of exosomes by using four exosomal protein marker antibodies: CD63, CD9, CD81, and HSP70.

NanoSight Particle Analysis

A NanoSight analysis was performed to determine sample particle size. Serum-derived exosomes isolated using ExoQuick were diluted. Analysis revealed particles with a mean diameter of 62 to 74 nm and total concentration of 2.33×10^{8} particles/ml (Fig. 5). Exosomes are known to lie within the range of 30 to 100 nm, so these data confirm that exosomes were present within the samples.

Apoptotic Effects of Purified Serum-Derived Exosomes of Patients With AMD

Markers of Apoptosis in Exosome-Treated ARPE-19 Cells

A Western blot analysis was performed to investigate the potential expression of Apaf-1, PARP, and caspase-3 in the exosome-treated ARPE-19 cell line.
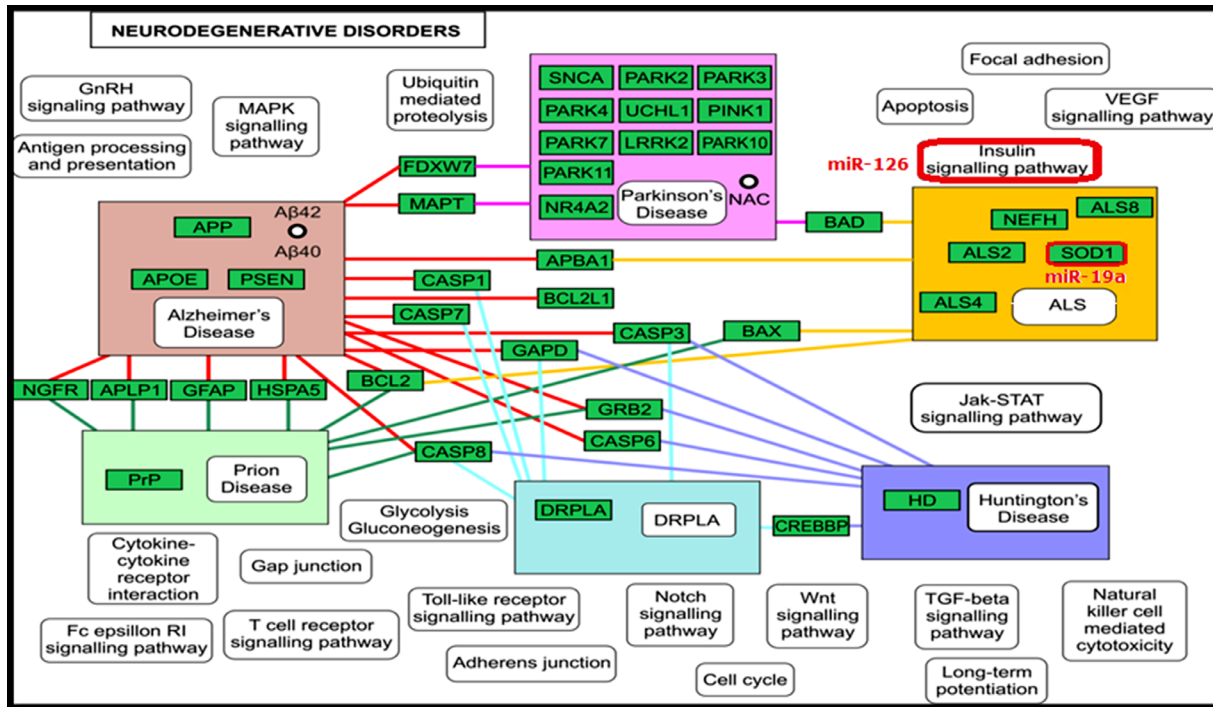
Figure 4. Neurodegenerative disorders signaling pathway and the predicted gene targets of miR-19a (SOD1) and miR-126, which are involved in the insulin signaling pathway. Core image from KEGG.

The anti–β-actin peroxidase was used as a positive control. ARPE-19 cells treated with AMD-derived exosomes showed significant expression, whereas ARPE-19 cells treated with control-derived exosomes or media only did not show significant expression for these protein markers. In addition, ImageJ densitometry software results showed the relative expression value of caspase-3 was significantly lower in ARPE-19

Table 1. Detected miRNA Target Genes and Signaling Pathways

| KEGG Pathways Enrichment in Target Genes	Target Genes
miR-410 has potential effects on 805 predicted target genes and is found in 173 signaling pathways, in which miR-410 is involved in retinal physiology/pathology	
Retinol metabolism	ALDH1A2
Apoptosis	NTRK1, IL1R1, PRKAR2B, PPP3CA, BIRC4
Nicotinate and nicotinamide metabolism	PBEF1
VEGF signaling pathway	KRAS, MAPK1, PPP3CA
Complement and coagulation cascades	CD55, PLAU
miR-19a has potential effects on 839 predicted target genes and is found in 166 signaling pathways, in which miR-19a is involved in retinal physiology/ pathology	
VEGF signaling pathway	PIK3CA, NFATC2, KRAS, SPHK2, PLA2G10, MAPK14, PIK3R3, RAF1
Apoptosis	PIK3CA, IL1R1, MAP3K14, PRKACB, PIK3R3
Complement and coagulation cascades	CR2, F3
miR-126 has potential effects on 22 predicted target genes and is found in 6 signaling pathways, in which miR-126 is involved in retinal physiology/pathology	
Cell communication	ITGA6
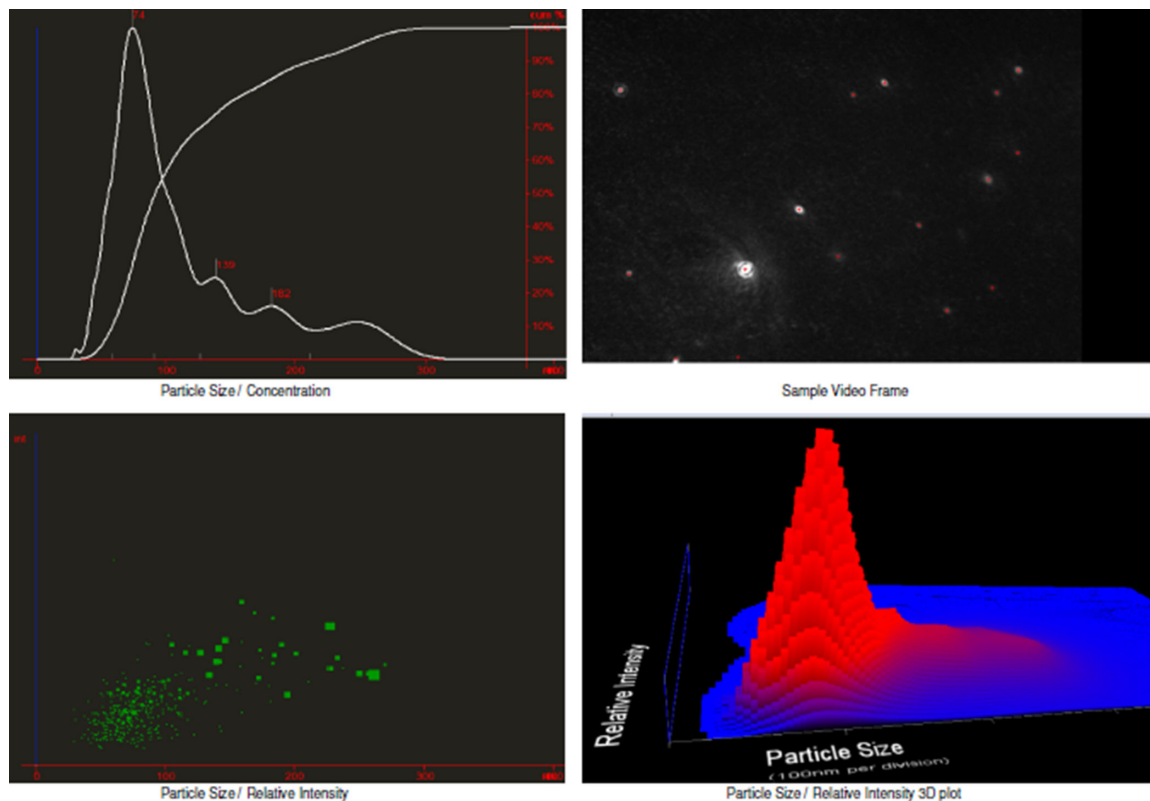
Figure 5. (**A**) Particle size/concentration. (**B**) Particle size/relative intensity 3D plot. Images show spherical vesicles between 30 and 100 nm, thus confirming the presence of exosomes. *Red arrow*: Exosomes particle.

cells treated with wet and dry AMD-derived exosomes than ARPE-19 cells treated with control-derived exosomes and media ($P = 0.001762$ and 0.000151 for dry and wet AMD, respectively) (Fig. 6). Although not significant, the expression of PARP in ARPE-19 cells treated with wet AMD-derived exosomes was higher compared with media only and control ($P = 0.0554$), as was the expression of Apaf-1 in ARPE-19 cells treated with dry AMD derived exosomes ($P = 0.053$).

Expression of Mature Apoptotic miRNA From ARPE-19 Cells Treated With Exosomes Derived From Patients With Dry or Wet AMD

In patients with AMD, evidence suggests that the RPE is lost via apoptosis.[33] The Human Apoptosis miScript miRNA PCR Array profiles the expression of 84 miRNAs that regulate programmed cell death (apoptosis). The functional gene grouping is shown in Supplementary Table S5.

The results show that, in comparison with the control group, dry AMD-derived exosomes affect the expression of the human apoptosis miRNAs let-7a-5p, miRNA-17-5p, miRNA195-5p, miRNA26b-5p, and miRNA-30c-5p more than wet AMD-derived exosomes (Fig. 7 and Table 2). Fold-regulation repre-

sents fold-change results in a biologically meaningful way. Fold-change values of less than 1 indicate a negative or downregulation, and the fold-regulation is the negative inverse of the fold-change. Fold-change values of greater than 1 indicate a positive or an upregulation, and the fold-regulation is equal to the fold-change. In Table 2, the fold-change and fold-regulation values greater than 2 are indicated with a *; fold-change values of less than 0.5 and fold-regulation values of less than –2 are indicated with a **. The *P* values are calculated based on a Student's *t*-test comparison of only two groups (dry vs. control and wet vs. control); *P* values of less than 0.05 are indicated with a *. This demonstrates a potential pathway of action of exosomes in the serum of affected patients with dry AMD.

The Effects of Serum-Derived Exosomes From Patients With AMD on an In Vitro Assay of Vasculogenesis and Angiogenesis

AMD-derived exosomes were shown to significantly induce angiogenesis and vasculogenesis in vitro compared with exosomes from the control samples. Tubule formation resulting from exposure to serum-derived exosomes from patients with dry AMD
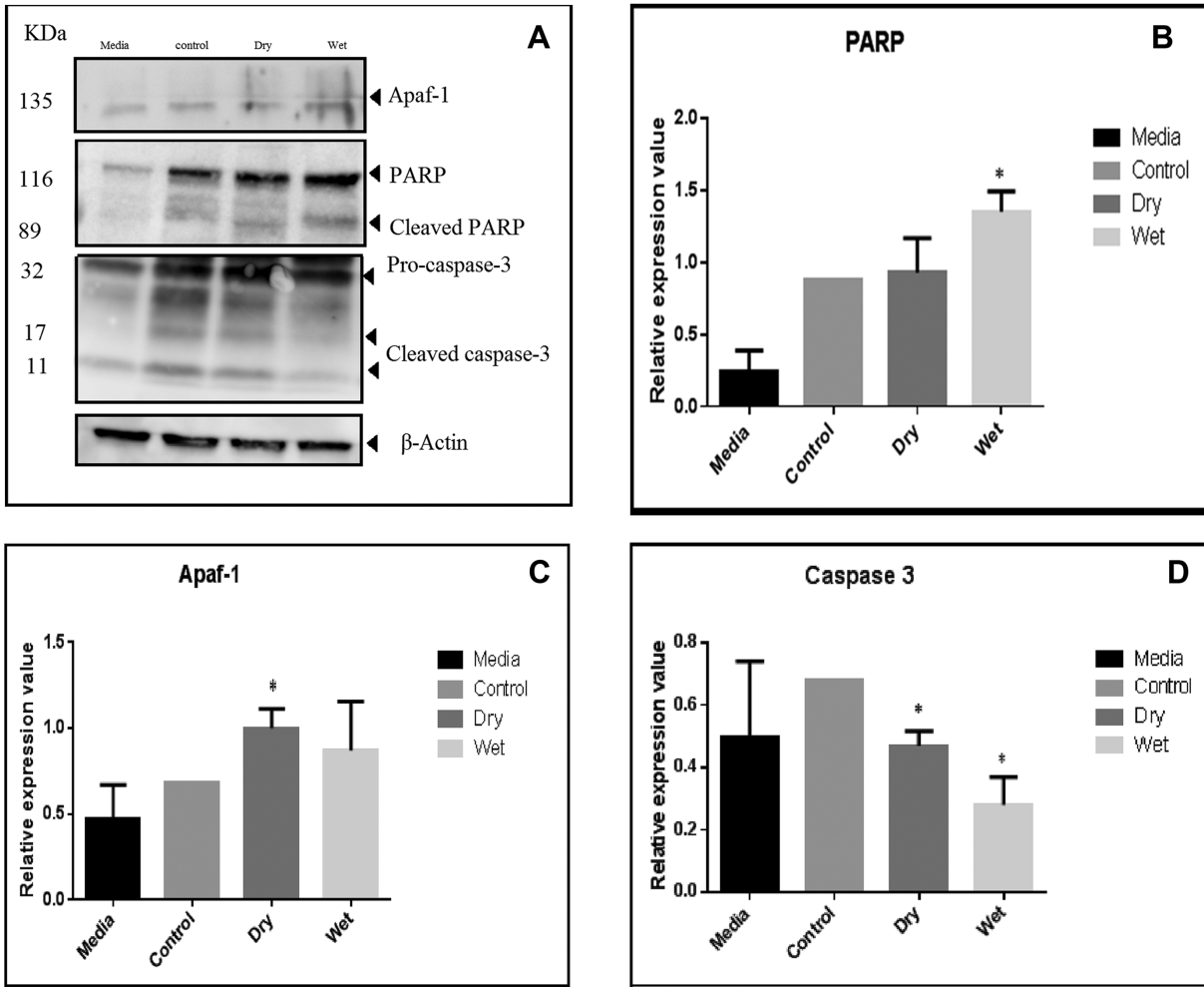
Figure 6. (**A**) Western blot for Apaf-1, PARP, and caspase-3 in exosome-treated ARPE-19 cell line. (**B**) ImageJ densitometry software results showing PARP expression in ARPE-19 cells treated with wet AMD-derived exosomes ($P = 0.0554$). (**C**) Apaf-1 expression in ARPE-19 cells treated with dry AMD-derived exosomes ($P = 0.053$). (**D**) The relative expression value of caspase-3 was significantly lower in ARPE-19 cells treated with wet and dry AMD-derived exosomes than ARPE-19 cells treated with control-derived exosomes and media ($P = 0.001$ for dry and 0.0002 for wet).
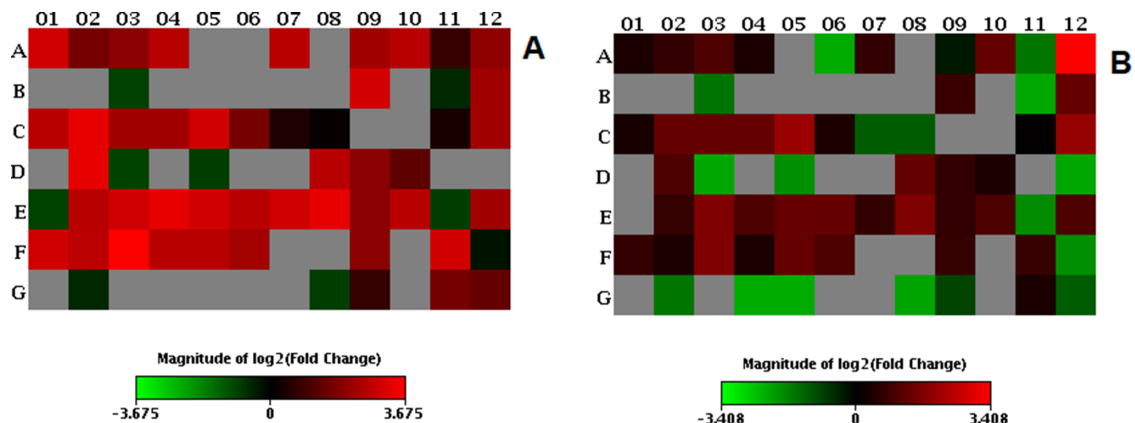

Figure 7. (A) Heat map of dry AMD versus control. (B) Heat map of wet AMD versus control. Heat maps define groups to report the fold-change results as a log transformation. *Red* indicates the upregulated miRNAs; *green* indicates downregulated miRNAs.

Table 2. Expression of miRNAs (That Regulate Apoptosis) From ARPE19 Cells After Exposure to Exosomes Extracted From Serum of Patients With "Wet" or "Dry" AMD

Mature ID	Fold Change Wet	Fold Change Dry	P Value Wet	P Value Dry	Upregulation or Downregulation Wet	Upregulation or Downregulation Dry
let-7a-5p	1.27	8.08*	0.5218	0.0256*	1.27	8.08*
let-7c	1.59	3.19*	0.1130	0.0267*	1.59	3.19*
let-7e-5p	2.01*	4.04*	0.0854	0.0199*	2.01*	4.04*
let-7g-5p	1.27	6.34*	0.5120	0.0000*	1.27	6.34*
hsa-miR-1	0.20**	0.50	0.0000*	0.0000*	-4.99**	-1.99
miR-101-3p	0.20**	0.50	0.0001*	0.0000*	-4.93**	-1.99
miR-106b-5p	1.59	6.42*	0.3481	0.0000*	1.59	6.42*
miR-122-5p	0.20**	0.50	0.0000	0.0000*	-4.99**	-1.99
miR-125a-5p	0.80	5.08*	0.4660	0.0000*	-1.25	5.08*
miR-125b-5p	2.53*	6.42*	0.0572	0.0000*	2.53*	6.42*
miR-128	0.34**	1.71	0.0123	0.0929	-2.96**	1.71
miR-1285-3p	10.62*	4.17*	0.1415	0.0828	10.62*	4.17*
miR-133a	0.20**	0.50	0.0000*	0.0000*	-4.99**	-1.99
miR-133b	0.20**	0.50	0.0000*	0.0000*	-4.99**	-1.99
miR-134	0.34**	0.52	0.0021*	0.0000*	-2.93**	-1.91
miR-141-3p	0.20**	0.50	0.0000*	0.0000*	-4.99**	-1.99
miR-143-3p	0.20**	0.50	0.0000*	0.0000*	-4.99**	-1.99
miR-144-3p	0.20**	0.50	0.0000*	0.0000*	-4.99**	-1.99
miR-145-5p	0.20**	0.50	0.0000*	0.0000*	-4.99**	-1.99
miR-146a-5p	0.20**	0.50	0.0000*	0.0000*	-4.99**	-1.99
miR-149-3p	1.67	8.35*	0.0976	0.0771	1.67	8.35*
miR-153	0.20**	0.50	0.0000*	0.0000*	-4.99**	-1.99
miR-15a-5p	0.21**	0.67	0.0001*	0.1709	-4.83**	-1.50
miR-15b-5p	2.53*	5.07*	0.0547	0.0197*	2.53	5.07*
miR-16-5p	1.26	6.37*	0.7873	0.0172*	1.26	6.37*
miR-17-5p	2.54*	10.08*	0.0531	0.0113*	2.54*	10.08*
miR-181a-5p	2.55*	5.07*	0.2578	0.0040*	2.55*	5.07*
miR-181b-5p	2.52*	5.03*	0.0546	0.0185*	2.52*	5.03*
miR-181c-5p	4.15*	8.23*	0.2340	0.0054*	4.15*	8.23*
miR-181d	1.29	3.24*	0.3539	0.0252*	1.29	3.24*
miR-183-5p	0.43**	1.34	0.0035*	0.3018	-2.35**	1.34
miR-185-5p	0.43**	1.07	0.0035*	0.0013*	-2.35**	1.07
miR-186-3p	0.20**	0.50	0.0000*	0.0000*	-4.99**	-1.99
miR-192-5p	0.20**	0.50	0.0000*	0.0000*	-4.99	-1.99
miR-193a-5p	1.01	1.26	0.9728	0.3771	1.01	1.26
miR-193b-3p	4.02*	5.05*	0.0476*	0.0040*	4.02*	5.05*
miR-194-5p	0.20**	0.50	0.0000*	0.0000*	-4.99	-1.99
miR-195-5p	2.03*	10.19*	0.0838	0.0000*	2.0*3	10.19*
miR-200c-3p	0.21**	0.51	0.0001*	0.0000*	-4.73**	-1.95
miR-203a	0.20**	0.50	0.0000*	0.0000*	-4.99**	-1.99
miR-204-5p	0.26**	0.54	0.0045*	0.0000*	-3.83**	-1.87
miR-205-5p	0.20**	0.50	0.0000*	0.0000*	-4.99**	-1.99
miR-206	0.20**	0.50	0.0000*	0.0000*	-4.99**	-1.99
miR-20a-5p	2.53*	6.42*	0.0541	0.0000*	2.53*	6.42*
miR-21-5p	1.59	4.02*	0.1125	0.0000*	1.59	4.02*
miR-210	1.30	2.58*	0.8002	0.1193	1.30	2.58*
miR-212-3p	0.20**	0.50	0.0000*	0.0000*	-4.99**	-1.99
miR-214-3p	0.21**	0.50	0.0001*	0.0000*	-4.73**	-1.99
miR-218-5p	0.20**	0.51	0.0000*	0.0000*	-4.99**	-1.95
miR-221-3p	1.61	6.40*	0.1067	0.0134*	1.61	6.40*
miR-222-3p	3.21*	8.07*	0.0521	0.0001*	3.21*	8.07*
miR-23a-3p	2.02*	10.18*	0.0820	0.0000*	2.02*	10.18*
miR-24-3p	2.57*	8.10*	0.0526	0.0243*	2.57*	8.10*
miR-25-3p	2.54*	6.41*	0.0525	0.0000*	2.54*	6.41*
miR-26a-5p	1.60	8.02*	0.1098	0.0000*	1.60	8.02*

Table 2. Continued

Mature ID	Fold Change Wet	Fold Change Dry	P Value Wet	P Value Dry	Upregulation or Downregulation Wet	Upregulation or Downregulation Dry
miR-26b-5p	3.19*	10.11*	0.1382	0.0117*	3.19*	10.11*
miR-27a-3p	1.60	4.02*	0.2422	0.0227*	1.60	4.02*
miR-29a-3p	2.03*	6.42*	0.1423	0.0000*	2.03	6.42*
miR-29b-3p	0.27**	0.54	0.0047*	0.0000*	-3.68**	-1.86
miR-29c-3p	2.03*	5.08*	0.0838	0.0000*	2.03	5.08*
miR-30a-5p	1.60	8.05*	0.1103	0.0000*	1.60	8.05*
miR-30b-5p	1.31	6.53*	0.4813	0.0000*	1.31	6.53*
miR-30c-5p	3.21*	12.78*	0.0242*	0.0101*	3.21	12.78*
miR-30d-5p	1.27	6.35*	0.5163	0.0000*	1.27	6.35*
miR-30e-5p	2.54*	6.42*	0.0527	0.0000*	2.54*	6.42*
miR-31-5p	2.03*	5.10*	0.0844	0.0000*	2.03*	5.10*
miR-32-5p	0.20**	0.50	0.0000*	0.0000*	-4.99**	-1.99
miR-338-3p	0.20**	0.50	0.0000*	0.0000*	-4.99**	-1.99
miR-34a-5p	1.61	4.01*	0.1049	0.0000*	1.61	4.01*
miR-34c-5p	0.20**	0.50	0.0000*	0.0000*	-4.99**	-1.99
miR-365b-3p	1.64	8.22*	0.1040	0.0000*	1.64	8.22*
miR-378a-3p	0.27**	0.84	0.0000*	0.5595	-3.76**	-1.19
miR-409-3p	0.20**	0.50	0.0000*	0.0000*	-4.99**	-1.99
miR-449a	0.34**	0.68	0.0111*	0.1807	-2.96**	-1.48
miR-451a	0.20**	0.50	0.0000*	0.0000*	-4.99**	-1.99
miR-491-5p	0.20**	0.50	0.0001*	0.0000*	-4.93**	-1.99
miR-497-5p	0.20**	0.50	0.0001*	0.0000*	-4.92**	-1.99
miR-512-5p	0.20**	0.50	0.0000*	0.0000*	-4.99**	-1.99
miR-542-3p	0.20**	0.50	0.0000*	0.0000*	-4.99**	-1.99
miR-7-5p	0.21**	0.54	0.0001*	0.0000*	-4.70**	-1.87
miR-708-5p	0.53	1.68	0.0000*	0.0988	-1.88	1.68
miR-9-5p	0.20**	0.50	0.0000*	0.0000*	-4.99**	-1.99
miR-92a-3p	1.26	3.19*	0.5203	0.0014*	1.26	3.19*
miR-98-5p	0.43**	2.70*	0.0037*	0.0603	-2.33**	2.70*

Fold change values, P value and fold regulation are compared with control.

*Fold-change and fold-regulation values of >2 are indicated. $P < 0.05$.

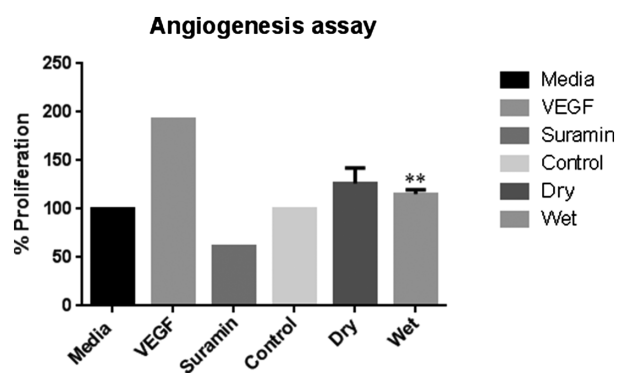**Fold-change values of <0.5 and fold-regulation values less than −2.

Figure 8. Graph representing the effects of serum-derived exosomes from patients with AMD on tubule formation compared with the effects of serum-derived exosomes from control patients. Dry, dry AMD samples; Suramin, negative control; Wet, wet AMD samples; VEGF, positive control. Wet AMD formed significantly more tubules ($n = 36$).
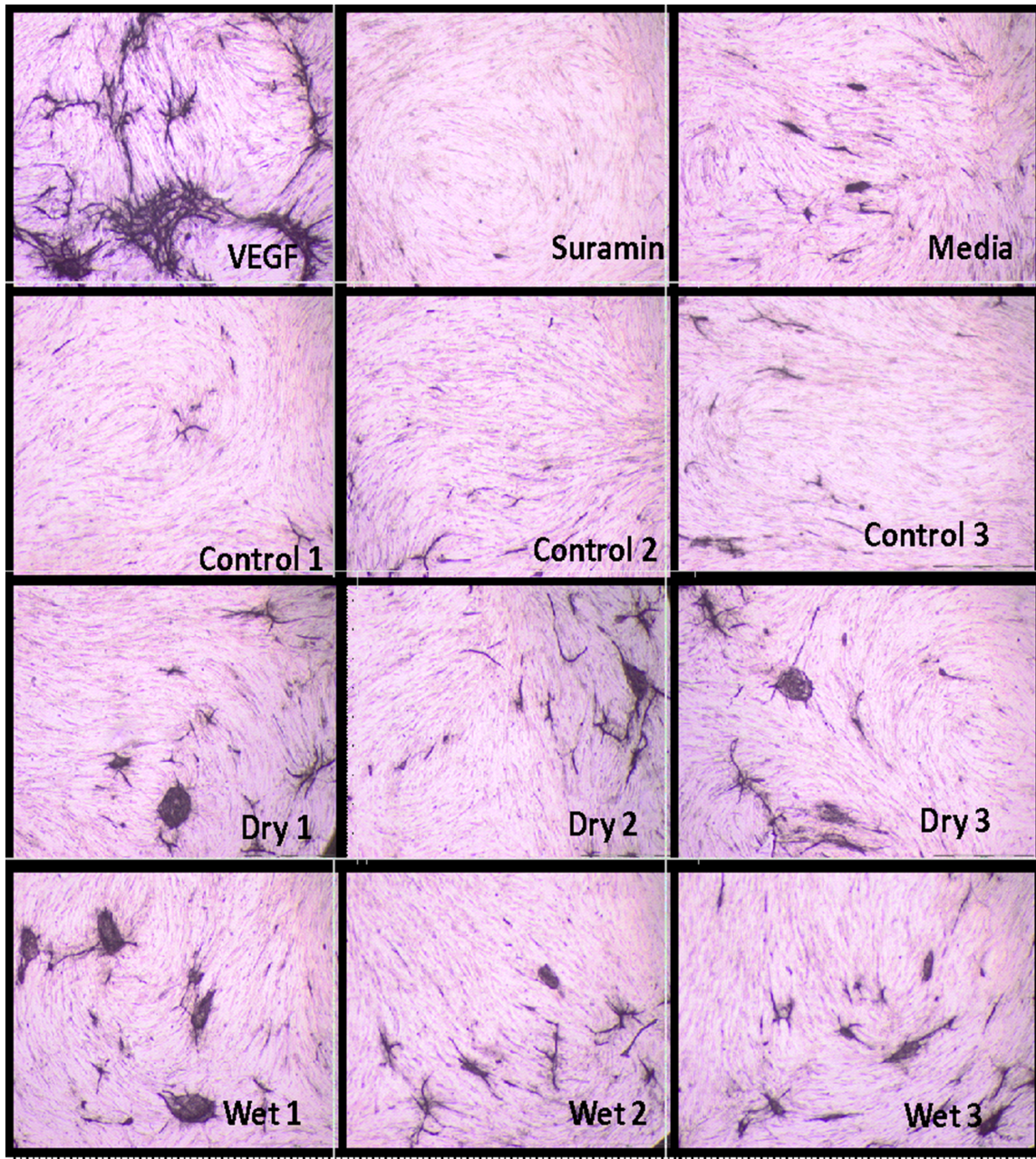
Figure 9. Tubule formation (indicated by red arrows) resulting from wet AMD serum-derived exosomes and dry AMD serum-derived exosomes, along with positive (VEGF) and negative (Suramin) controls ($n = 36$).

suggest the presence of specific miRNAs (angiomiRs) in that stage of AMD, despite the absence of neovascular manifestation in the eye. However, wet AMD-derived exosomes significantly induce angiogenesis and vasculogenesis in vitro compared with exosomes from controls. The results show that 10 µg of serum-derived exosomes from wet patients with AMD form significantly more tubules ($P = 0.002$) (Figs. 8 and 9).

To confirm the previous results, the tubule-like structures were analyzed using TCS Cellworks AngioSys Image Analysis Software (ZHA-6000). AMD serum-derived exosomes were found to affect tubule formation in comparison with control serum-derived exosomes, suggesting the important role of miRNAs in angiogenesis in patients with AMD (Fig. 10, Table 3).
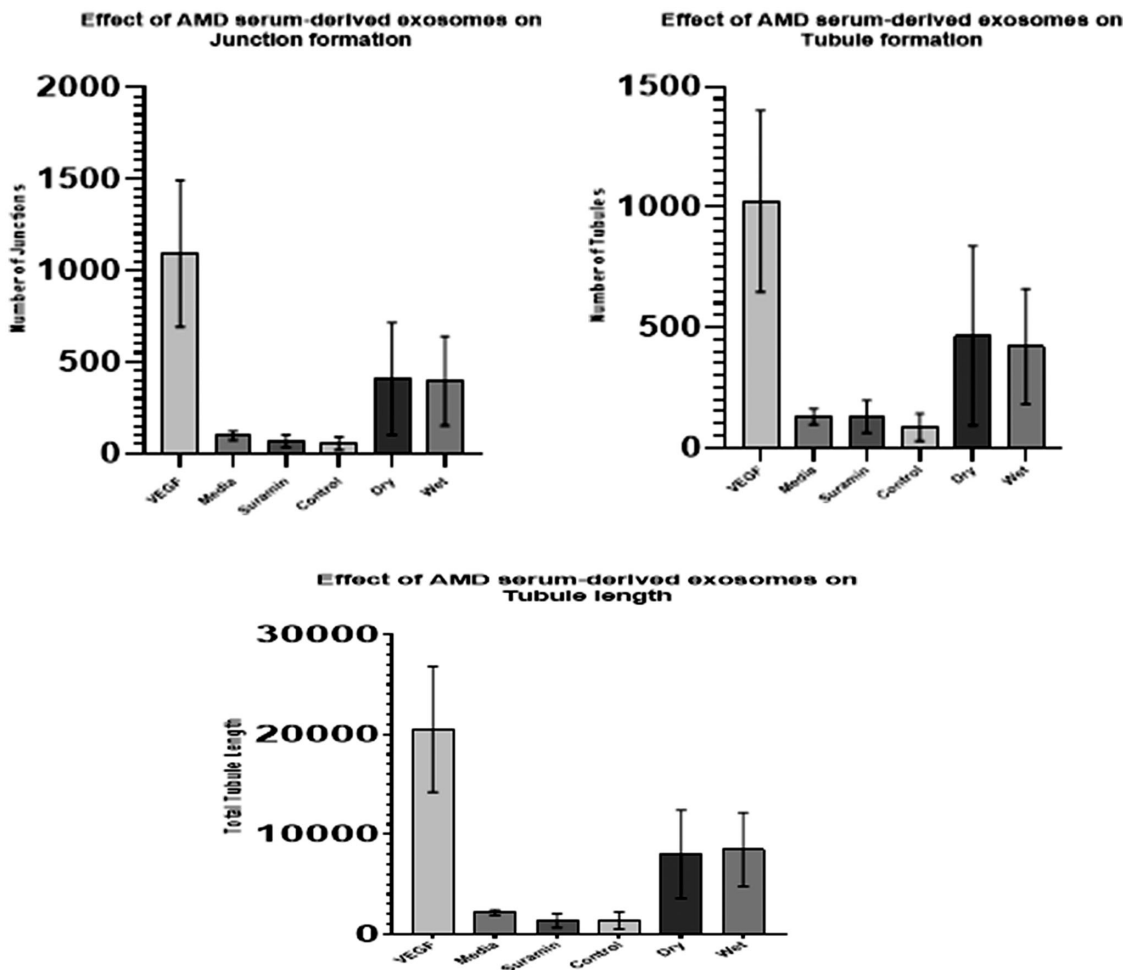
Figure 10. Effect of AMD serum-derived exosomes on endothelial tubule formation, determined by using a V2a AngioKit and serum-derived exosomes from wet AMD and dry patients with AMD. VEGF = positive control. Suramin = negative control. Results were significant for wet AMD and dry AMD (P [analysis of variance] = 0.0006, 0.0017, and 0.0001). Data represent mean values $\pm$ SD ($*P \leq 0.05$, $**P \leq 0.01$, $***P \leq 0.001$).

Table 3. Average of Junctions, Tubules, and Total Tubule Length among 2 Plates to Evaluate the Effect of AMD Serum-Derived Exosomes on Endothelial Tubule Formation by Applying Serum-Derived Exosomes from Wet AMD and Dry Patients with AMD

Treatment	Average Junctions	Average Tubules	Average Total Tubule Length
VEGF	1091 $\pm$ 199	1024 $\pm$ 188	20,539 $\pm$ 3147
Media	99 $\pm$ 11	129 $\pm$ 16	2173 $\pm$ 132
Suramin	68 $\pm$ 34	128 $\pm$ 67	1350 $\pm$ 692
Wet	396 $\pm$ 121	420 $\pm$ 119	8477 $\pm$ 1851
Control	55 $\pm$ 17	84 $\pm$ 28	1359 $\pm$ 426
Dry	409 $\pm$ 153	465 $\pm$ 186	8018 $\pm$ 2203
Analysis of variance *P* value	**0.0006**	**0.0017**	**0.0001**
Wet vs. control	8.42559E-05	0.00010213	1.57608E-06
Dry vs. control	0.000628985	0.00201673	3.76705E-05

Suramin and VEGF were used for the negative and positive control, respectively. Data are mean values $\pm$ SD.

Discussion

The identification of AMD-related miRNAs will be essential for assisting the diagnosis and treatment of AMD. Our discoveries of miRNA function in AMD by using in vitro human ARPE-19 cells and angiogenesis models may be applicable for future development of cell-based therapies for AMD.

This study provides preliminary evidence to support the involvement of AMD-derived exosomes, as miRNA cargo, in the pathology of AMD. It also revealed the role of miRNAs in apoptosis and angiogenesis, which are mediated by cell-to-cell communication mechanisms through exosomes. AMD-derived exosomes, as miRNA carriers, have the ability to affect ARPE-19 cells, thus resulting in the increased expression of apoptosis protein markers, induction of cell death and over-expression of human apoptosis miRNAs. AMD-derived exosomes may also induce angiogenesis in in vitro human angiogenesis endothelial models.

VEGF plays a causal role in the development of choroidal neovascularization by increasing angiogenesis and vascular permeability.[34] As our results showed, some miRNAs are related to the VEGF signaling pathway, namely miR-410 and miR-19-a. The underlying mechanism of how miR-410 targets VEGF-A, and the potential for treatment of retinal neovascularization, have been previously demonstrated.[35] miR-126 also shows proangiogenic and antiangiogenic function in the vasculature of both endothelial cells and perivascular cells.[36] Nevertheless, in pathologic conditions such as inflammation, the similar angiogenic signaling pathway is misregulated.[37,38] miR-126 seems to have an important role in blood vessel development by enhancing VEGF signaling, angiogenesis, and vascular integrity.[36]

Extracellular deposits are a hallmark of many neurodegenerative conditions, including AD.[39,40] Dry AMD is associated with extracellular lipid, protein, and complement deposition termed drusen. This type of deposit is also present in numerous degenerative retinal diseases, such as glaucoma and AMD, which are considered to be neurodegenerative diseases.[41] Our bioinformatics analysis showed that miR-410 and miR-19a are associated with the apoptosis signaling pathway. miR-19a belongs to the miR-17~92 cluster.[35,42] This cluster has an important role in apoptosis and angiogenesis.[43] One previous report showed that overexpression of the entire miR-17~92 cluster increases angiogenesis and vascular growth, which reveals the potential proangiogenic effect of miR-19a.[44] Further evidence supporting the correlation between miR-19 and angiogenesis was demonstrated by Dews et al.,[45] who found that miR-19a was correlated with decreased expression of several antiangiogenic factors such as thrombospondin-1 and connective tissue growth factor.[45] miR-19a and miR-19b also play important roles during neurogenesis and cell regulation, and they are involved in the pathways that regulate cell proliferation, differentiation, and apoptosis.[46]

Cigarette smoking is a modifiable risk factor for AMD development and progression.[47] It provokes dysregulation of miRNA through genetic or epigenetic damage to miRNAs, such as the P53 pathway. P53 is a tumor suppressor protein that can induce cell cycle arrest, cell growth, apoptosis, and angiogenesis.[48] According to the results of this study, the predicted miRNA target pathways of miR-410 are involved in retinol metabolism and nicotinate and nicotinamide metabolism signaling pathways. In addition, altered retinoid homeostasis is a potential mechanism for smoking-associated toxicities. It has been demonstrated that nornicotine, a nicotine metabolite and component of cigarette smoke, catalysis retinals. Nornicotine-catalyzed retinal isomerization is involved in the molecular mechanism for AMD.[49] A recent study on the effect of environmental tobacco smoke on circulatory miRNAs identified six miRNAs as circulatory candidate miRNAs in AMD (let-7a, let-7c, miR-106a-5p, miR-106b-5p, miR-17-5p, and miR-361-5p).[50] It also demonstrated that environmental tobacco smoke extract has a stimulatory effect on VEGF expression through the Toll-like receptor 4/reactive oxygen species/mitogen-activating protein kinase/nuclear factor-kappaB signaling pathway.

Vascular integrity is believed to be maintained by cell signaling mechanisms between endothelial cells, endothelial progenitor cells, and stromal cells. Exosomes are essential as mediators for intracellular communication.[51] Thus, exosomes play a role in the mediation of angiogenesis; endothelial cell–derived exosomes have been shown to stimulate migration and angiogenesis in recipient cells.[52] The role of miR-214 exosome mediation between endothelial cells has previously been demonstrated.[53] This implies that exosomes may have the ability to influence the recipient endothelial cells by inducing angiogenesis, as shown in our results for the vasculogensis to angiogenesis human in vitro model.

The results of exosome interaction with the in vitro RPE model showed that AMD-derived exosomes interact with ARPE-19 cells and have the ability to transfer their apoptotic capability to them. PARP cleavage, Apaf-1, and caspase-3 are considered to be apoptosis markers[54]; a Western blot analysis showed that PARP is highly expressed in ARPE-19 cells treated with wet AMD-derived exosomes, whereas Apaf-1 was

expressed in ARPE-19 cells treated with dry AMD-derived exosomes. However, the relative expression value of caspase-3 was lower in ARPE-19 cells treated with wet and dry AMD-derived exosomes than ARPE-19 cells treated with control-derived exosomes and media.

Human apoptosis miRNA PCR array profiling results provide evidence that dry AMD-derived exosomes affect the expression of human apoptosis miRNAs more than wet AMD-derived exosomes in comparison with control group. let-7a-5p, miRNA-17-5p, miRNA195-5p, miRNA26b-5p, and miRNA-30c-5p showed higher expression in the APRE-19 cells, which were treated with dry AMD-derived exosomes, which supports the previous research that identified strong roles for apoptosis in dry AMD.[55] The upregulation of miRNA-23a/miRNA-27a, miRNA-34a, and miRNA-125b-1 with exosomes from serum of patients with dry AMD and not wet AMD demonstrates potential mechanism of local effect of serum exosomes which corroborates some of the findings of Pogue et al and Hill et al in AD.[17,18] Note that the other local miRNA detailed by this group (miRNA-7, miRNA-9-1, and miRNA-146a) are also upregulated by exosomes from the serum of patients with wet and dry AMD. Exosomes play a role in cell-to-cell communication activity, thus affecting recipient cells, and they are also proving to play a pivotal role in apoptosis.[56]

Exosomes play a key role in intercellular communication; this provides a promising mechanism of intercellular communication mediated by secretory miRNAs.[57] Further studies are required to identify the role of extracellular exosomes and their effect on intracellular (RPE) function in AMD. This might give rise to new therapeutic approaches, for example, inhibiting AMD-derived exosome function. Therefore, extracellular vesicles are essential mediators and regulators which may have novel therapeutic applications.

The identification of target genes and potential mechanism of circulating miRNAs in AMD has undoubtedly shown great promise for their application in a clinical setting. However, there is a risk of false-positive prediction with the current computational methods, because they still lack sensitivity and specificity, which is one of the main limitations of this study.[58] Indeed this is a limitation of all miRNA studies in AMD. It is difficult to illicit a clear cause/effect profile from miRNA expression and disease. This can be attributable to the differential effects of miRNAs in different tissues and from different origins, that is, local versus systemic.

The impact of purified exosomes on an in vitro model demonstrated here illustrates that to a certain extent. Our in vitro studies provided preliminary evidence that AMD-derived exosomes (containing miRNAs) may play a key role in AMD pathology and might offer novel diagnostic and therapeutic approaches for AMD.

It is also important to acknowledge our very basic classification of AMD in this patient cohort (dry [non-neovascular] or wet [neovascular]). Recent work by global experts illustrate the challenge in truly classifying AMD and if it really is a spectrum of disease or a heterogenous group of disorders.[59] Furthermore, the challenges for accurate detection of universal miRNA biomarkers in AMD are that miRNAs differential expression or dysregulation were shown to present variability according to race and ethnic groups.[60–62] However, the data on the race and ethnicity variation of miRNA profiles in different cases of AMD are scarce.[63] The data presented here are from a Caucasian population and we accept there will be miRNA variability when this analytic approach is applied to other ethnic groups. Also, the dry and wet AMD forms presented here are at a point in time. We have not yet specifically looked at a prospective AMD cohort that convert to wet type. That will be the subject of further studies. The previous studies show little overlap in the finding of miRNA biomarkers to distinguish AMD types.[63] This is likely as a result of the heterogeneity of AMD and the difficulty in assigning a clear classification to AMD subtypes.

Currently, there are no effective treatments available for dry AMD or geographic atrophy. Meanwhile, VEGF inhibition therapy is the best available treatment for wet AMD, although the frequency of administration of anti-VEGF intravitreal injections is burdensome for these patients. miRNA biomarkers might provide targets for the development of novel therapeutic options.[64,65] Recent studies suggest the role of anti-miRNA based therapeutics in neurodegenerative disorders such AD. Therefore, targeted anti-miRNA and/or combinatorial approaches could become useful in the clinical management of AMD and in other neurodegenerative disorders.[66,67] Ahead of trials, we would propose waiting until a clear reproducible list of target miRNAs are identified in serum and/or retina/RPE from multiple research groups. The lack of good animal models for non-neovascular AMD hampers this approach.[68]

In conclusion, this study has identified the pathologic role of the discovered miR-19a, miR-126 and miR-410 in AMD. It also described the functional roles of miRNAs in in vitro human cell line models through AMD-derived exosomes. The results may be applicable to development of therapies for AMD.

Acknowledgments

References

1. Li JQ, Welchowski T, Schmid M, Mauschitz MM, Holz FG, Finger RP. Prevalence and incidence of age-related macular degeneration in Europe: a systematic review and meta-analysis. *Br J Ophthalmol*. 2019;104(8):1077–1084.

2. Strauss O. The retinal pigment epithelium in visual function. *Physiol Rev*. 2005;85(3):845–881.

3. Ao J, Wood, JP, Chidlow, G, Gillies, MC, Casson, RJ. Retinal pigment epithelium in the pathogenesis of age-related macular degeneration and photobiomodulation as a potential therapy? *Clin Exp Ophthalmol*. 2018;46(6):670–686.

4. Inui M, Martello G, Piccolo S. MicroRNA control of signal transduction. *Nat Rev Mol Cell Biol*. 2010;11(4):252–263.

5. O'Brien J, Hayder, H, Zayed, Y, Peng, C. Overview of MicroRNA biogenesis, mechanisms of actions, and circulation. *Front Endocrinol (Lausanne)*. 2018;9:402.

6. Ha TY. MicroRNAs in human diseases: from cancer to cardiovascular disease. *Immune Netw*. 2011;11(3):135–154.

7. Soifer HS, Rossi J.J., Saetrom P. MicroRNAs in disease and potential therapeutic applications. *Mol Ther*. 2007;15(12):2070–2079.

8. Thai TH, Christiansen PA., Tsokos GC. Is there a link between dysregulated miRNA expression and disease? *Discov Med*. 2010;10(52):184–194.

9. Wang S, Koster, KM, Yuguang, H, Zhou, Q. miRNAs as potential therapeutic targets for age-related macular degeneration. *Future Med Chem*. 2012;4(3):277–287.

10. Elbay A, Ercan, C, Akbaş, F, Bulut, H, Ozdemir, H. Three new circulating microRNAs may be associated with wet age-related macular degeneration. *Scand J Clin Lab Invest*. 2019;79(6):388–394.

11. Romano GL, Platania, CBM, Drago, F, et al. Retinal and circulating miRNAs in age-related macular degeneration: an in vivo animal and human study. *Front Pharmacol*. 2017;8:168.

12. Huntley RP, Kramarz, B, Sawford, T, et al. Expanding the horizons of microRNA bioinformatics. *RNA*. 2018;24(8):1005–1017.

13. Li L, Xu, J, Yang, D, Tan, X, Wang, H. Computational approaches for microRNA studies: a review. *Mamm Genome*. 2010;21(1-2):1–12.

14. Hsu SD, Lin, FF, Wu, WY, et al. miRTar-Base: a database curates experimentally validated microRNA-target interactions. *Nucleic Acids Res*. 2011;39(Database issue):D163–D169.

15. Makarev E, Cantor, C, Zhavoronkov, A, Buzdin, A, Aliper, A, Csoka, AB. Pathway activation profiling reveals new insights into age-related macular degeneration and provides avenues for therapeutic interventions. *Aging*. 2014;6(12):1064–1075.

16. Lukiw WJ, Alexandrov, PN, Zhao, Y, Hill, JM, Bhattacharjee, S. Spreading of Alzheimer's disease inflammatory signaling through soluble microRNA. *Neuroreport*. 2012;23(10):621–626.

17. Pogue AI, Lukiw WJ. Up-regulated pro-inflammatory MicroRNAs (miRNAs) in Alzheimer's disease (AD) and age-related macular degeneration (AMD). *Cell Mol Neurobiol*. 2018;38(5):1021–1031.

18. Hill JM, Pogue AI, Lukiw WJ. Pathogenic microRNAs common to brain and retinal degeneration; recent observations in Alzheimer's disease and age related macular degeneration. *Front Neurol*. 2015;6:232–232.

19. Cornel S, Adriana, ID, Mihaela, TC, et al. Anti-vascular endothelial growth factor indications in ocular disease. *Rom J Ophthalmol*. 2015;59(4):235–242.

20. Lin H, Qian, J, Castillo, AC, et al. Effect of miR-23 on oxidant-induced injury in human retinal pigment epithelial cells. *Invest Ophthalmol Vis Sci*. 2011;52(9):6308–6314.

21. Wang AL, Lukas, TJ, Yuan, M, Du, N, Tso, MO, Neufeld, AH. Autophagy and exosomes in the aged

retinal pigment epithelium: possible relevance to drusen formation and age-related macular degeneration. *PLoS One*. 2009;4(1):e4160.

22. van Niel G, Porto-Carreiro, I, Simoes, S, Raposo, G. Exosomes: a common pathway for a specialized function. *J Biochem*. 2006;140(1):13–21.

23. Mathivanan S, Ji H, Simpson RJ. Exosomes: extracellular organelles important in intercellular communication. *J Proteomics*. 2010;73(10):1907–1920.

24. Roccaro AM, Sacco, A, Maiso, P, et al. BM mesenchymal stromal cell-derived exosomes facilitate multiple myeloma progression. *J Clin Invest*. 2013;123(4):1542–1555.

25. Maia J, Caja, S, Strano Moraes, MC, Couto, N, Costa-Silva, B. Exosome-based cell-cell communication in the tumor microenvironment. *Front Cell Dev Biol*. 2018;6:18.

26. Wang AL, Lukas, TJ, Yuan, M, Du, N, Tso, MO, Neufeld, AH. Autophagy, exosomes and drusen formation in age-related macular degeneration. *Autophagy*. 2009;5(4):563–564.

27. Lee JK, Park, SR, Jung, BK, et al. Exosomes derived from mesenchymal stem cells suppress angiogenesis by down-regulating VEGF expression in breast cancer cells. *PLoS One*. 2013;8(12):e84256.

28. Rana S, Malinowska K, Zoller M. Exosomal tumor microRNA modulates premetastatic organ cells. *Neoplasia*. 2013;15(3):281–295.

29. Neelam K, Hogg, RE, Stevenson, MR, et al. Carotenoids and co-antioxidants in age-related maculopathy: design and methods. *Ophthalmic Epidemiol*. 2008;15(6):389–401.

30. ElShelmani H, Wride, MA, Saad, T, Rani, S, Kelly, DJ, Keegan, D. Identification of novel serum microRNAs in age-related macular degeneration. *Transl Vis Sci Technol*. 2020;9(4):28–28.

31. Vlachos IS, Zagganas, K, Paraskevoopoulou, MD, et al. DIANA-miRPath v3.0: deciphering microRNA function with experimental support. *Nucleic Acids Res*. 2015;43(W1):W460–W466.

32. Yu LL, Zhu, J, Liu, JX, et al. A comparison of traditional and novel methods for the separation of exosomes from human samples. *Biomed Res Int*. 2018;2018:3634563.

33. Kaarniranta K, Tokarz, P, Koskela, A, Paterno, J, Blasiak, J. Autophagy regulates death of retinal pigment epithelium cells in age-related macular degeneration. *Cell Biol Toxicol*. 2017;33(2):113–128.

34. Churchill AJ, Carter, JG, Lovell, HC, et al. VEGF polymorphisms are associated with neovascular age-related macular degeneration. *Hum Mol Genet*. 2006;15(19):2955–2961.

35. Chen N, Wang, J, Hu, Y, et al. MicroRNA-410 reduces the expression of vascular endothelial growth factor and inhibits oxygen-induced retinal neovascularization. *PLoS One*. 2014;9(4):e95665.

36. Nikolic I, Plate KH, Schmidt MH. EGFL7 meets miRNA-126: an angiogenesis alliance. *J Angiogenes Res*. 2010;2(1):9.

37. Anand S, Cheresh DA. Emerging role of microRNAs in the regulation of angiogenesis. *Genes Cancer*. 2011;2(12):1134–1138.

38. Cantaluppi V, Gatti, S, Medica, D, et al. Microvesicles derived from endothelial progenitor cells protect the kidney from ischemia-reperfusion injury by microRNA-dependent reprogramming of resident renal cells. *Kidney Int*. 2012;82(4):412–427.

39. Kaarniranta K, Salminen, A, Haapasalo, A, Soininen, H, Hiltunen, M. Age-related macular degeneration (AMD): Alzheimer's disease in the eye? *J Alzheimers Dis*. 2011;24(4):615–631.

40. Wang L, Clark, ME, Crossman, DK, et al. Abundant lipid and protein components of drusen. *PLoS One.* 2010;5(4):e10329.

41. Landa G, Butovsky, O, Shoshani, J, Schwartz, M, Pollack, A. Weekly vaccination with Copaxone (glatiramer acetate) as a potential therapy for dry age-related macular degeneration. *Curr Eye Res*. 2008;33(11):1011–1013.

42. Todoerti K, Barbui, V, Pedrini, O, et al. Pleiotropic anti-myeloma activity of ITF2357: inhibition of interleukin-6 receptor signaling and repression of miR-19a and miR-19b. *Haematologica*. 2010;95(2):260–269.

43. Xu XL, Jiang, YH, Feng, JG, Su, D, Chen, PC, Mao, WM. MicroRNA-17, microRNA-18a, and microRNA-19a are prognostic indicators in esophageal squamous cell carcinoma. *Ann Thorac Surg*. 2014;97(3):1037–1045.

44. Doebele C, Bonauer, A, Fischer, A, et al. Members of the microRNA-17-92 cluster exhibit a cell-intrinsic antiangiogenic function in endothelial cells. *Blood*. 2010;115(23):4944–4950.

45. Dews M, Homayouni, A, Yu, D, et al. Augmentation of tumor angiogenesis by a Myc-activated microRNA cluster. *Nat Genet*. 2006;38(9):1060–1065.

46. Marcuzzo S, Kapetis, D, Mantegazza, R, et al. Altered miRNA expression is associated with neuronal fate in G93A-SOD1 ependymal stem progenitor cells. *Exp Neurol*. 2014;253(1090-2430 (Electronic)):91–101.

47. Govindaraju VK, Bodas M, Vij N. Cigarette smoke induced autophagy-impairment regulates

AMD pathogenesis mechanisms in ARPE-19 cells. *PLoS One*. 2017;12(8):e0182420.

48. Russ R, Slack FJ, Cigarette-smoke-induced dysregulation of microRNA expression and its role in lung carcinogenesis. *Pulm Med*. 2012;2012: 791234.

49. Brogan AP, Dickerson, TJ, Boldt, GE, Janda, KD. Altered retinoid homeostasis catalyzed by a nicotine metabolite: implications in macular degeneration and normal development. *Proc Natl Acad Sci U S A*. 2005;102(30):10433–10438.

50. Smit-McBride Z, Nguyen, J, Elliott, GW, et al. Effects of aging and environmental tobacco smoke exposure on ocular and plasma circulatory microRNAs in the Rhesus macaque. *Mol Vis*. 2018;24:633–646.

51. Su SA, Xie, Y, Fu, Z, Wang, Y, Wang, JA, Xiang, M. Emerging role of exosome-mediated intercellular communication in vascular remodeling. *Oncotarget*. 2017;8(15):25700–25712.

52. Ribeiro MF, Zhu, H, Millard, RW, Fan, GC. Exosomes function in pro- and anti-angiogenesis. *Curr Angiogenes*. 2013;2(1):54–59.

53. van Balkom BW, de Jong, OG, Smits, M, et al. Endothelial cells require miR-214 to secrete exosomes that suppress senescence and induce angiogenesis in human and mouse endothelial cells. *Blood*. 2013;121(19):3997–4006.

54. Zhang F, Lau SS, Monks TJ. A dual role for poly(ADP-ribose) polymerase-1 during caspase-dependent apoptosis. *Toxicol Sci*. 2012;128(1):103–114.

55. Huang P, Sun, J, Wang, F, et al. MicroRNA expression patterns involved in amyloid beta-induced retinal degeneration. *Invest Ophthalmol Vis Sci*. 2017;58(3):1726–1735.

56. Yang L, Wu, XH, Wang, D, Luo, CL, Chen, LX. Bladder cancer cell-derived exosomes inhibit tumor cell apoptosis and induce cell proliferation in vitro. *Mol Med Rep*. 2013;8(4):1272–1278.

57. Kosaka N, Iguchi, H, Yoshioka, Y, Takeshita, F, Matsuki, Y, Ochiya, T. Secretory mechanisms and intercellular transfer of microRNAs in living cells. *J Biol Chem*. 2010;285(23):17442–17452.

58. Min H, Yoon S, Got target? Computational methods for microRNA target prediction and their extension. *Exp Mol Med*. 2010;42(4):233–244.

59. Klein R, Meuer, SM, Myers, CE, et al. Harmonizing the classification of age-related macular degeneration in the three-continent AMD consortium. *Ophthalmic Epidemiol*. 2014;21(1):14–23.

60. Rawlings-Goss RA, Campbell MC, Tishkoff SA. Global population-specific variation in miRNA associated with cancer risk and clinical biomarkers. *BMC Med Genomics*. 2014;7:53.

61. Restrepo NA, Spencer, KL, Goodloe, R, et al. Genetic determinants of age-related macular degeneration in diverse populations from the PAGE study. *Invest Ophthalmol Vis Sci*. 2014;55(10):6839–6850.

62. Huang RS, Gamazon, ER, Ziliak, D, et al. Population differences in microRNA expression and biological implications. *RNA Biol*. 2011;8(4):692–701.

63. Martinez B, Peplow PV. MicroRNAs as diagnostic and prognostic biomarkers of age-related macular degeneration: advances and limitations. *Neural Regen Res*. 2021;16(3):440–447.

64. Maroñas O, García-Quintanilla, L, Luaces-Rodríguez, A, et al. Anti-VEGF treatment and response in age-related macular degeneration: disease's susceptibility, pharmacogenetics and pharmacokinetics. *Curr Med Chem*. 2020;27(4):549–569.

65. Zhao Y, Alexandrov PN, Lukiw WJ. Anti-microRNAs as novel therapeutic agents in the clinical management of Alzheimer's disease. *Front Neurosci*. 2016;10:59.

66. Jaber VR, Zhao, Y, Sharfman, NM, Li, W, Lukiw, W. Addressing Alzheimer's disease (AD) neuropathology using anti-microRNA (AM) strategies. *Mol Neurobiol*. 2019;56(12):8101–8108.

67. Bhattacharjee S, Zhao, Y, Dua, P, Rogaev, EI, Lukiw, WJ,et al. microRNA-34a-mediated down-regulation of the microglial-enriched triggering receptor and phagocytosis-sensor TREM2 in age-related macular degeneration. *PloS One*. 2016;11(3):e0150211–e0150211.

68. Pennesi ME, Neuringer M, Courtney RJ. Animal models of age related macular degeneration. *Mol Aspects Med*. 2012;33(4):487–509.